Journal of Manufacturing Engineering, March 2019, Vol. 14, Issue. 1, pp 010-025

A COMPARATIVE STUDY TO EVALUATE THE CORROSION PERFORMANCE OF FRICTION STIR WELDED AZ31B MAGNESIUM ALLOY UNDER IMMERSION, SALT FOG, PITTING AND GALVANIC CORROSION TESTS UNDER NACL ENVIRONMENT

https://doi.org/10.37255/jme.v4i1pp010-025

***Ashok Kumar M[1], Thirumalaikumarasamy D[2], Paventhan R[3] and Thirumal P[4]**

[*] Department of Mechanical Engineering, MRK Polytechnic College, Kattumannarkoil – 608301
[2,4]Department of Mechanical Engineering, Government College of Engineering, Bargur– 635104
[3]Department of Mechanical Engineering, Karpaga Vinayagar College of Engineering And Technology, Chennai– 600024

ABSTRACT

An investigation was carried out to quantify and characterize the corrosion behaviour of AZ31B magnesium alloy joints. Extruded Mg alloy plates of 6 mm thick of AZ31B grade were butt welded using a solid state, environmentally cleaner welding process, friction stir welding process. The weld specimens were underwent immersion, salt spray, pitting and galvanic corrosion tests in order to quantify and characterize the corrosion rates of the welds with the influence of different pH values, chloride ion concentration and the corrosion time. The corrosion rates, microstructure, scanning electron microscopy and X-ray diffraction analysis concludes the optimum parameter for the usage of the magnesium alloy welds for the best service applications. Keywords: Keywords: EDM, Alumina and Genetic Algorithm

Keywords: *AZ31B magnesium alloys, Friction stir welding, Corrosion tests, Scanning electron microscopy and X-ray Diffraction.*

1. Introduction

Magnesium alloy developments have traditionally been driven by aerospace and automobile industry requirements for lightweight materials to operate under increasingly demanding conditions. Magnesium alloys have always been attractive to designers due to their low density, only two thirds that of aluminium. This has been a major factor in the widespread use of magnesium alloy castings and wrought products [1,2]. The better joining of magnesium components made from this alloy, is however still limited. Unfortunately, conventional fusion welding of magnesium alloys often produces porosity, hot cracks etc., in the welded joint. This deteriorates both the mechanical properties as well as corrosion resistance [3, 4]. Hence, it will be of extreme benefit if a solid state joining process can be developed and implemented for the joining of magnesium alloys.

So in this research work, the joints were made by friction stir welding process (FSW). It is a solid state welding process without emission of ration or dangerous fumes and it avoids the formation of solidification defects like hot cracking and porosity. In addition, it significantly improved the weld properties and had been extensively applied in joining of magnesium alloys and aluminum alloys [5].

However, the corrosion resistances of the Mg-based alloys are generally inadequate due to the low standard electrochemical potential or free corrosion potential -2.37 V compared to the SHE (Standard Hydrogen Electrode) [6] and this limits the wide range of applications for Mg and its alloys. Therefore, the studies of corrosion behavior of magnesium alloys are important in active media to choose the best optimum corrosion parameters for various service applications.

It aims to facilitate research directed at Mg alloy development and at understanding corrosion of Mg alloy and its friction stir welds in service applications to ensure such research is as effective as possible, where the pH value, chloride ion concentration and corrosion time as the corrosion parameters. This research focused a comparison among immersion corrosion, salt spray corrosion, pitting corrosion and galvanic corrosion, which are the four main techniques for the corrosion studies in an effort to expose the magnesium alloy and its welds to environments similar to those environments experienced for service applications. From the literature review, it was understood that most of the published information on corrosion behavior of Mg alloys were focused on general corrosion and pitting corrosion of unwelded base alloys. Very few investigations have

**Corresponding Author - E- mail: ashokleadsaero12@gmail.com*

been conducted so far on corrosion behavior of FSW joints of Mg alloys and particularly there are a few publications on combination of four corrosion tests in FSW AZ31B Mg alloy welds corrosion. The aim of this research is to investigate the occurrence of corrosion quantitatively and the corrosion characterization of friction stir welded AZ31B magnesium alloy for service applications with the propitious to study the effect of pH value, chloride ion concentration and corrosion time on corrosion rate of AZ31B magnesium alloy welds.

2. Experimental Procedure

2.1 Test Materials

The material used in this study was AZ31B magnesium alloy in the form of extruded condition and supplied in plates of 6 mm thickness. The chemical composition and mechanical properties of the base metal are presented in Table 1(a) & 1(b).

Table 1(a), Chemical composition (wt %) of AZ31B Mg alloy

Al	Zn	Mn	Mg
5.45	1.26	0.17	Balance

Table 1(b).Mechanical properties of AZ31B Mg alloy

Yield Strength (MPa)	Ultimate Tensile Strength (MPa)	Elongation (%)	Vickers hardness at 0.05 kg load (Hv)
177	272	8	57

The optical micrograph of base metal is shown in Fig.1; it was observed that the microstructure of base metal contains coarse grains with $Al_{12}Mg_{17}$ intermetallic compounds. The intermetallic compounds scattered adjacent to the grain boundaries.

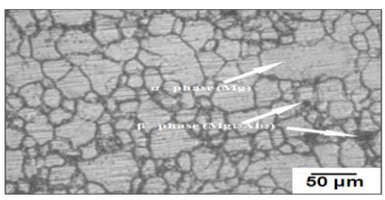

Fig.1 Optical micrograph of AZ31B base metal.

2.2 Fabricating the joints and preparing the test specimens

An indigenously designed and developed computer numerical controlled friction stir welding machine (22kW; 4000 RPM; 60kN) was used to fabricate joints. The FSW parameters were optimized by conducting trial runs and the welding conditions which produced defect free joints were taken as optimized welding conditions. The optimized welding conditions used to fabricate the joints in this investigation are presented in Table. 2. The pin is having threaded profile with 1 mm pitch.

Table 2 Optimized Welding conditions and process parameters used to fabricate the joints.

Rotational speed (rpm)	Welding speed (mm/min)	Axial force (kN)	Tool shoulder diameter, (mm)	Pin diameter, (mm)	Pin length, (mm)
1000	75	3	18	6	5

The welded portion (Stir zone) was extracted from the fabricated plates were used for corrosion tests and characterization survey. The welded specimens were ground with $500^{\#}$, $800^{\#}$, $1200^{\#}$, $1500^{\#}$ grit SiC paper. Finally, it was cleaned with acetone and washed in distilled water then dried by warm flowing air. The optical micrograph of the stir zone of the FSW joint of AZ31B magnesium alloy is shown in Fig.2; here, it reveals that the stir zone contains fine grains with significantly refined $Al_{12}Mg_{17}$ intermetallic compounds. The size of the refined $Al_{12}Mg_{17}$ are sharply around 8-15 µm after welding. However the β-phases are refined which are not uniformly distributed in the magnesium matrix. This may varies the rate of corrosion.

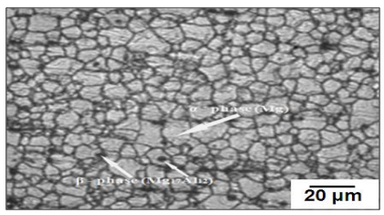

Fig. 2 Optical micrograph of stir zone of FSW AZ31B Mg alloy

2.3 Finding the limits of corrosion test parameters

From the literature [7, 8 and 9], the predominant factors that have a greater influence on corrosion behavior of AZ31B magnesium alloy are identified. Based on the literature studies and systematic experimental works were conducted using trial and error method (runs). They are: (i) pH value of the solution, (ii) exposure time and (iii) chloride ion concentration. Large numbers of trial experiments were conducted to identify the feasible testing conditions using friction stir welded AZ31B magnesium alloy joints.

2.4 Experimental Design Matrix

Owing to a wide range of factors, the use of three factors and central composite rotatable design matrix was chosen to minimize number of experiments. The assay conditions for the reaction parameters were taken at zero level (center point) and one level (+1 and (1). The design was extended up to a ±α (axial point) of 1.68. The center values for variables were carried out at least six times for the estimation of error and single runs for each of the other combinations; twenty runs were done in a totally random order. The design would consist of the eight corner points of the 23cube, the six star points, and m center points [10]. The star points would have a = 8^ (1/4) = 1.682. Design matrix consisting of 20 sets of coded conditions (comprising a full replication three factorial of 8 points, six corner points and six centre points) was chosen in this investigation. Table 3 represents the ranges of factors considered, and Table 4, shows the 20 sets of coded and actual values used to conduct the experiments. For the convenience of recording and processing experimental data, the upper and lower levels of the factors were coded here as +1.682 and -1.682 respectively. The coded values of any intermediate value could be calculated using following relationship

$$Xi=1.682[2X–(X_{max}-X_{min})]/(X_{max}-_{min}) \quad \text{..... (1)}$$

where,

X_i is the required coded value of a variable X and X is any value of the variable from X_{min} to X_{max};

X_{min} is the lower level of the variable;

X_{max} is the upper level of the variable.

Table 3 Important factors and their levels

Sl.No.	Factor	Unit	Notation	Levels				
				-1.682	-1	0	+1	+1.682
1	pH value		P	3	4.62	7	9.38	11
2	Exposure time	hours (h)	T	1	2.62	5	7.38	9
3	Cl^- Concentration	Mole(M)	C	0.2	0.36	0.6	0.84	1

Table 4 Design matrix and Experimental test results

Expt. No	Input parameters (Coded Values)			Corrosion rate (mm/yr)			
	pH	Time (h)	Cl^- (M)	Immersion corrosion test	Salt spray corrosion test	Pitting corrosion test	Galvanic corrosion test
1	4.62	2.62	0.36	6.32	14.62	3.98	0.047

2	9.38	2.62	0.36	4.62	10.23	2.54	0.030
3	4.62	7.38	0.36	4.63	11.89	3.39	0.034
4	9.38	7.38	0.36	3.99	8.99	2.14	0.011
5	4.62	2.62	0.84	9.60	15.82	4.56	0.058
6	9.38	2.62	0.84	5.62	11.31	4.25	0.035
7	4.62	7.38	0.84	8.43	12.92	5.19	0.052
8	9.38	7.38	0.84	6.65	10.75	3.76	0.032
9	3	5	0.60	6.60	17.96	6.41	0.059
10	11	5	0.60	3.65	8.88	2.68	0.020
11	7	1	0.60	6.21	11.23	5.20	0.061
12	7	9	0.60	4.36	8.51	4.30	0.027
13	7	5	0.20	4.45	8.66	4.21	0.018
14	7	5	1	8.95	15.28	6.91	0.053
15	7	5	0.60	5.96	9.80	5.00	0.041
16	7	5	0.60	5.96	9.89	5.00	0.043
17	7	5	0.60	5.96	9.89	5.00	0.043
18	7	5	0.60	5.96	9.89	5.00	0.043
19	7	5	0.60	5.96	9.89	5.00	0.043
20	7	5	0.60	5.96	9.89	5.00	0.043

3. Corrosion testing

The corrosion behaviour of AZ31B magnesium alloy welds were characterized by four different corrosion tests like immersion corrosion, salt spray corrosion, pitting corrosion and galvanic corrosion tests. Solution of NaCl with concentrations of 0.2M, 0.36M, 0.6M, 0.84M, and 1M were prepared and the pH value of the solution was used as pH 3, pH 4.62, pH 7, pH 9.38, & pH 11 with concentrated HCl and NaOH respectively for all the four tests. As the corrosion rate of magnesium alloys were extremely high, the corrosion tests were performed for smaller time durations of 1, 2.62, 5, 7.38 and 9 hours. The working surface for the corrosion evaluation were (for immersion corrosion, hydrogen gas collection, salt fog, potentio-dynamic polarisation curves, galvanic corrosion) were mechanically ground to 1200 grit SiC paper, washed with distilled water and dried with warm flowing air.

The immersion corrosion testing was enhanced as per the ASTM norms G-31 and evaluating the corrosion tested specimen with the method as per ASTM G1. The corrosion rate was measured using weight loss method. The salt spray corrosion tests method consists of exposing the specimens in a salt spray chamber as per

ASTM B 117 standards and evaluating the corrosion tested specimen with the method as per ASTM G1-03. The pitting corrosion testing was carried out as per ASTM G5. Electrochemical polarization tests were performed using a potentiostat GILL AC interfaced to a personal computer. All the potentials referred in this paper are with respect to SCE. A platinum foil served as a counter electrode. The electrodes for this purpose were prepared by connecting a wire to one side of the sample that was covered with cold setting resin. Prior to polarization experiments, the free corrosion potential (FCP) was monitored and the experiments were begun after stabilization of FCP. All the results were triplicate so as to ensure reproducibility of the test results. The specimens were exposed and a polarizations scan was carried out towards more noble values at a rate 18 mV/min. The scan scope was set from -2000 mV to 0 mV vs. OCP (Open Circuit Potential). All electrochemical tests were conducted in triplicates in order to ensure the reproducibility of results. The corrosion potential was developed and observed from the open circuit potential.. The corrosion current density (i_{corr}) was estimated at the intersection point of extrapolated cathodic polarization curve and the horizontal line drawn at zero current potential. The galvanic currents flowing between equal areas of friction stir welded AZ31B magnesium alloy welds coupled with AZ31B magnesium alloy base metal were obtained by the zero resistance ammeter (ZRA) technique. The ZRA experiments were performed, which pure samples of equal areas were kept at a distance of 6 mm. When the mixed potential theory was applied to the individual reactions, the coupled corrosion rates were i_{corr} (PA/PA) for AZ31B magnesium alloy base metal and i_{corr} (WZ/WZ) for AZ31B friction stir welds. Thus the current i_{corr} (PA/WZ) was the galvanic current which can be measured by a (ZRA) Zero Resistance Ammeter. Also it was assumed that the current distributed uniformly across the area used in this calculation.

3.1 Corrosion rate measurement

The simplest and most fundamental measurement of the corrosion rate is the metal weight loss rate, ΔW (mg/cm^2/d). This can be converted to an average corrosion rate (mm/y) using [11, 12, 13, 14]

Corrosion rate (weight loss measurements)

$$CR_w = \frac{8.76 \times 10^4 \times w}{A \times D \times T} \text{ mm/y} \quad \text{(2)}$$

where,

w = weight loss in grams.

A = surface area of the specimen in cm^2

D = density of the material, 1.72 g/cm^3

T = corrosion time in hours.

In the overall corrosion reaction of pure Mg, one molecule of hydrogen is evolved for each atom of corroded Mg. One mol (i.e. 24.31 g) of Mg metal corrodes for each mol (i.e. 22.4 L) of hydrogen gas produced. Therefore, the hydrogen evolution rate, V_H (ml/cm^2/d), is related to the metallic weight loss rate, ΔW, using [15, 16, 17]

$$\Delta W = 1.085\ V_H \text{ mm/yr} \quad \text{(3)}$$

The corresponding corrosion rate, CR_H, is evaluated by substituting Eq. (4) into Eq. (2) to give

$$CR_H = 2.279\ V_H \text{ mm/yr} \quad \text{(4)}$$

For Mg corrosion, there is excellent agreement between the corrosion rate measured by the weight loss rate and that evaluated from the hydrogen evolution rate. In the pitting corrosion test and galvanic corrosion tests for measuring the corrosion rate, the corrosion current density i_{corr} (mA/cm^2) is estimated from the Potentio-dynamic polarization curve, and i_{corr} is related to the average corrosion rate using [18]

Corrosion rate (Potentiodynamic polarization & ZRA measurements),

$$CR_i = 22.85\ i_{corr} \text{ mm/yr} \quad \text{(5)}$$

From the literature review, it was observed that, why this electrochemical technique might not give reliable values for Mg corrosion. Nevertheless the electrochemical technique of polarization test is widely used for the evaluation of the corrosion of Mg alloys, at least partly, because it is a quick and easy technique. Therefore it is useful to review the literature on this technique for Mg alloys. It is useful to have quantitative measures of the quality of the corrosion rate evaluated by the potentiodynamic polarization technique. The corrosion test results for all the corrosion tests was recorded in the Table 4.

3.2 Metallography

Micro structural examination of the corroded specimens was carried out using a light optical microscope (Union Opt. co. ltd. Japan; Model: VERSAMET-3) incorporated with an image analyzing software (Clemex-vision). The exposed specimen surface was prepared for the micro examination with minor polish. The corrosion test specimens were polished in disc polishing machine for scratch free surfaces. To determine the depth and diameter of the pit, the exposed specimens were cut in cross sectional, the corrosion products were removed, then the specimens were covered with cold setting resin and the surface was observed at 200X magnification.

4. Developing an Empirical Relationship

The response surface methodology (RSM) approach was adopted in this study because of its following advantages: (1) the ability to evaluate the effects of interactions between tested parameters; (2) the benefit of limiting the number of actual experiments to be carried out, in comparison to a classical approach for the same number of estimated parameters [19, 20]. In the present investigation, to correlate the potentiodynamic polarization tests parameters and the corrosion rate of AZ31B welds, a second order quadratic model was developed. The response (corrosion rate of AZ31B welds) is a function of pH values (P), exposure time (T) and chloride ion concentration (C) and it could be expressed as,

Corrosion rate = f (P, T, C) …….. (6)

The Analysis of Variance (ANOVA) technique was used to find the significant main and interaction factors. The results of second order response surface model fitting as Analysis of Variance (ANOVA) for all the four corrosion tests are given in the Table 5. The determination coefficient (r^2) indicates the goodness of fit for the model. Values of "Prob > F" less than 0.0500 indicated model terms were significant. In this case P, T, C, PT, TC, T^2 are significant model terms for immersion corrosion test; P, T, C, P^2, C^2 are the significant model terms for salt spray corrosion test; P, T, C, PT, TC, C^2 are significant model terms for pitting corrosion test and P, T, C, TC, T^2 are significant model terms for galvanic corrosion test. All this indicated an excellent suitability of the regression model.

4.1 Checking the adequacy of the model

Table 5 ANOVA test results

Source	Immersion corrosion test		Salt spray corrosion test		Pitting corrosion test		Galvanic corrosion test	
	F value	**p-value Prob>F**	**F value**	**p-value Prob>F**	**F value**	**p-value Prob>F**	**F value**	**p-value Prob>F**
Model	29.22*	<0.0001	27.04*	<0.0001	38.65*	<0.0001	27.66*	<0.0001
P	27.7*	0.0004	91.08*	<0.0001	74.98*	<0.0001	92.93*	<0.0001
T	195.19*	<0.0001	10.37*	0.0092	28.34*	0.0003	10.64*	0.0085
C	10.88*	0.0080	116.31*	<0.0001	196.08*	<0.0001	117.12*	<0.0001
PT	6.54*	0.0285	4.60	0.0577	7.54*	0.0206	4.67	0.0559
PC	0.98	0.3461	4.65	0.0564	3.55	0.0890	4.73	0.0547
TC	4.93	0.0507	5.58*	0.0398	15.64*	0.0027	5.67*	0.0385
P^2	2.39	0.1534	5.31*	0.0440	0.12	0.7385	2.82	0.1238
T^2	12.23*	0.0057	3.49	0.0915	0.84	0.3807	6.51*	0.0287
C^2	0.57	0.4686	0.91	0.3634	19.56*	0.0013	3.09	0.1091
Lack of Fit	0.1238		0.2893		0.1311		0.1805	

Std. Dev.	0.54	0.67	0.42	3.15×10^{-3}
Mean	5.79	11.44	0.46	0.037
R^2	0.9418	0.9657	0.9605	0.9611
Adj. R^2	0.8894	0.9349	0.9203	0.9260
Pred. R^2	0.6413	0.8176	0.7636	0.7745

* Values of "Prob > F" less than 0.0500 indicate that the model terms are significant

5. Results and Discussion

Table 4, shows the corrosion rate of all the four corrosion tests. This data shows that the weight loss evaluated from immersion and salt spray corrosion tests agrees within an error of ±10% with the rate independently measured from hydrogen evolution for both the tests. The hydrogen evolution was measured and found that the corrosion initiated as localized corrosion at some sites on the surface and subsequently expanded over the whole surface. The hydrogen evolution, after an initiation time of several hours, increased linearly with exposure time. The advance of the corrosion over the surface of friction stir welds of AZ31B was slower, although the corrosion also initiated as localized corrosion. The hydrogen evolution, after an initiation time of several hours, increased with exposure time. For most alloys, the rate of hydrogen evolution initially increased with increasing exposure time, which is attributed to corrosion occurring over increasing fractions of the surface as was observed.

The possibility of galvanic corrosion occurrence was investigated using zero resistance ammetry techniques in order to measure the galvanic couple potential and galvanic couple current densities between couple electrodes. The couple electrodes were selected in two categories: identical electrodes which were the connection of two identical electrodes from weld zone, named WZ/WZ and identical electrodes of from parent alloy named PA/PA. Another couple electrode set up was selected from two non-identical electrodes, one from weld zone and the other from parent alloy, which is named here as PA/WZ. All the galvanic measurements were carried out at room temperature. The reason of choosing identical couple electrodes was to compare the measured current density of these couples and the current density which is measured from two non-identical electrodes. Bearing in mind that theoretically there is no driving force for galvanic corrosion occurrence between two identical electrodes where two electrodes are completely identical from the morphological point of view and chemical composition. Any difference between the two electrodes due to chemical composition or morphology can cause a galvanic cell formation leads to generation of current from anode of the cell to the cathode.

From the above tests result, the difference in the corrosion potential between the PA/PA and WZ/WZ is found to be -90mV, providing the results that the couple seems to be galvanically corrosive resistant.. From the obtained results, the corrosion rates of galvanic couple was in the range of 0.03-0.06 mm/yr, which is quite negligible and shows excellent property of corrosion resistant as per corrosion hand books and guides. So, the galvanic couple can be suitable for good applications [21, 22 and 23].

On a note on microstructure, all second phases have the tendency to cause micro-acceleration of the corrosion of the alpha-Mg matrix [15, 16 and 17], so a multi-phase alloy has typically a corrosion rate greater than that of pure Mg. The second phase can provide a barrier effect if it is essentially continuous and has a lower corrosion rate than the alpha-Mg matrix; otherwise there is the tendency for the corrosion rate to be accelerated, even for second phase particles as small [24]. It was observed that, Mg alloys like AZ31B, the corrosion is caused by the beta phase accelerating the corrosion of the adjacent Mg alpha phase. The acceleration of the overall corrosion rate can be by a factor of 0–20 [25]. It was found that the mechanical properties and the corrosion resistance of FSW Mg alloys are higher or equivalent to the base material from the literature [26, 27]. The corrosion resistance in the weld was higher than in the base material owing to the fact that the weld possesses finer grains than the base alloy.

5.1 Effect of pH on corrosion rate

As it can see that, both immersion and salt spray corrosion tests shows a linear trend towards weight loss. But, on comparing the weight loss between

the two tests, interestingly salt spray corrosion tests posses greater weight loss than the immersion corrosion tests. However, some recent literature, proved that, immersion corrosion tests posses greater weight loss. But in this case, the salt spray corrosion tests having greater weight loss when compared with immersion corrosion tests. This is due to the spraying effect, where non recylcling of solution were done. This means inorder to maintain a proper functional results, the spraying was done without recycle the solution thereafter. [28]. It is suspected that, the weight loss is the removing magnesium from the welds. However, due to the aggressiveness of the solution, the welds loss more magnesium.

On comparison, the corrosion rates among the four corrosion tested specimen were represented as bar diagram in the Fig. 3. It was found that, the corrosion rates obtained from the four corrosion tests was in the order of salt spray corrosion test > Immersion corrosion test > Potentiodynamic polarization test > Galvanic corrosion tests. There is a substantial increase in the pH of the solution during its exposure causing alkalization or basification of the solution with the increase of reactivity and time. On the other hand, exposure conditions of potentiodynamic polarization test prevails the continuous presence of water, resulted in the removal of corrosion by-products and the removal of surrounding magnesium, meaning that the pit area would decreased in the exposed surface of the specimen during polarization test. First, the removal of the corrosion products on the exposed surface of polarization test would reduce the ability to of the pits to continue growing, as the corrosion products trap chloride ions within the pits.

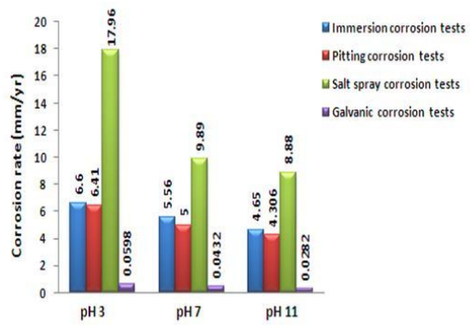

Fig. 3 Comparative estimation of corrosion rate with respect to pH value.

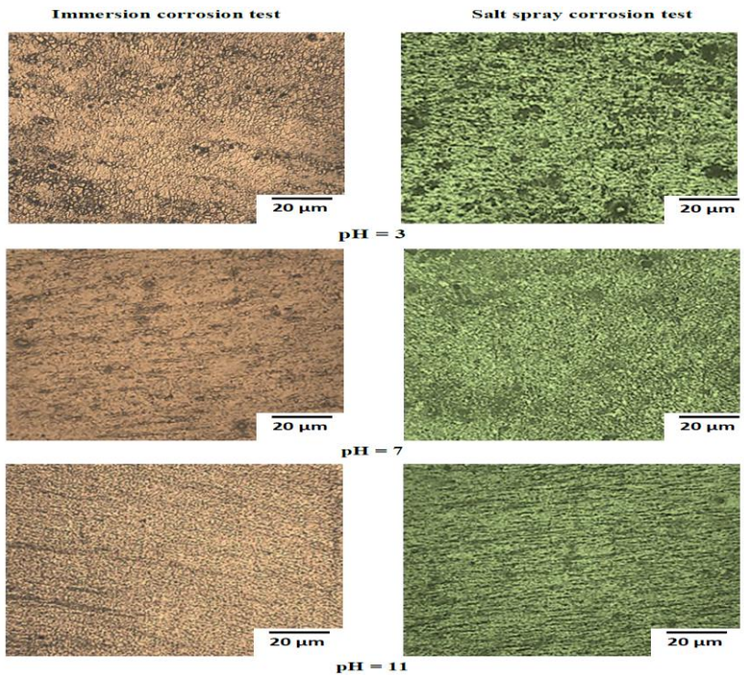

Fig. 4 Effect of pH on Pit Morphology for immersion corrosion tests and salt spray corrosion tests.

Fig. 4 shows the effect of pH on pit morphology of the corroded specimen exposed in 0.6M concentration of NaCl for 5 hours with different pH values of pH 3, pH 7 and pH 11 for immersion corrosion tests and salt spray corrosion tests. During salt spray testing and immersion corrosion tests, the density of the pit formed in exposing lower pH (acidic) solution is quite high, comparing with the neutral and alkaline solution. It was observed that the matrix shows the pitting marks and the pitting corrosion that has taken place at the friction stir welded microstructure. The particles are Mn-Al compound (Precipitate) and fragmented $Mg_{17}Al_{12}$ precipitated along the magnesium matrix.

The numbers of pits were more in the joints when it is immersed or sprayed with the solution of low pH.. Hence the corrosion rate increases with the decrease in pH value. Since the increase in the number of grain and grain boundary in the joints, the grain boundary acts cathodic to grain causing micro galvanic effect. The presence of micro-galvanic effect between the α-phase and the β-phase, formed due to the presence of aluminum. However, the finer grains reduce the corrosion rate, but in this case of friction stir welds the corrosion rate was increased. This is due to the microgalvanic effect of α-phase and the β-phase particle. The β-phase mainly served as a galvanic cathode found along the grain boundaries and accelerated the corrosion process of the α-matrix.

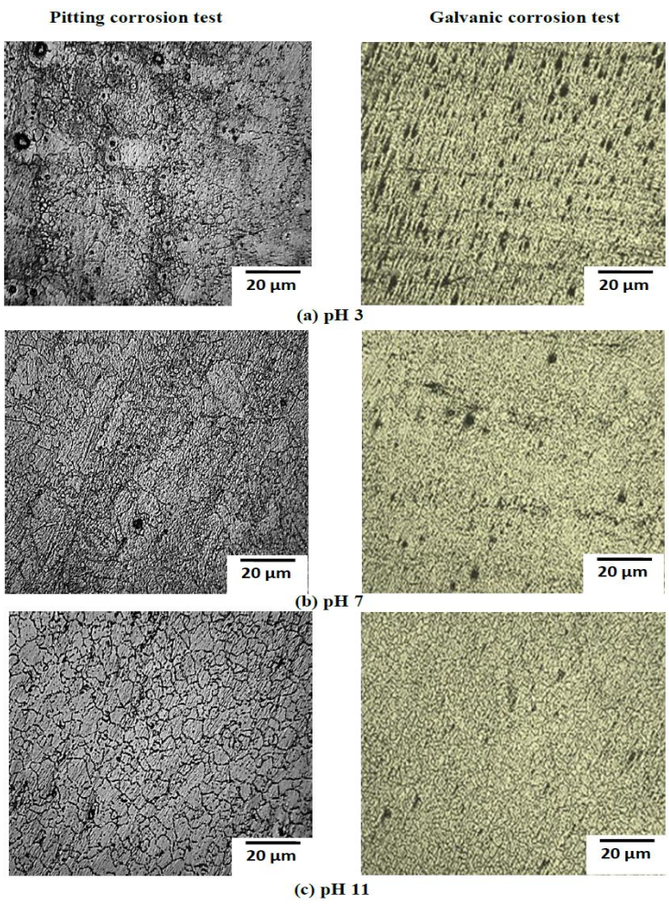

Fig. 5 Effect of pH on Pit Morphology for Pitting corrosion tests and galvanic corrosion tests.

Fig. 5 shows the effect of pH on pit morphology of the corroded specimen exposed in 0.6M concentration of NaCl for 5 hours with different pH values of pH 3, pH 7 and pH 11 for pitting corrosion

tests and galvanic corrosion tests. During polarization test, the grain boundaries of the specimen get attacked and its gravity varies with the parameters used in the experiment. Corrosion tends to be concentrated in the area adjacent to the grain boundary until eventually the grain may be undercut and fall out [29]. It was observed from the pit morphological observation of galvanic corrosion specimen (anodic), the density of the pit formed in exposing lower pH (acidic) solution is quite high, comparing with the neutral and alkaline solution in the anodic specimen. In FS welds, the grain boundaries get attacked and its gravity varies with the parameters used in the experiment**.** Fewer pits were found in the base metal since it was cathodic to the anodic AZ31B welds. In anode, the anodic dissolution is under activation control. Thus, the cathodic specimen was less attacked throughout the tests.

5.2 Effect of chloride ion concentration on corrosion rate

On comparison, the corrosion rates among the four corrosion tested specimen were represented as bar diagram in the Fig. 6. This is consistent with the detailing of the protective layer. With the increase of chloride ion concentration, the initial protective layer changed into soluble $MgCl_2$ layer for salt spray corrosion and $Mg(OH)Cl_2$ for immersion corrosion and electrochemical corrosion. The corrosion rate was quite higher in salt spray corrosion test than the immersion and polarization test. It states that, the $MgCl_2$ was highly soluble compared to $Mg(OH)Cl_2$.

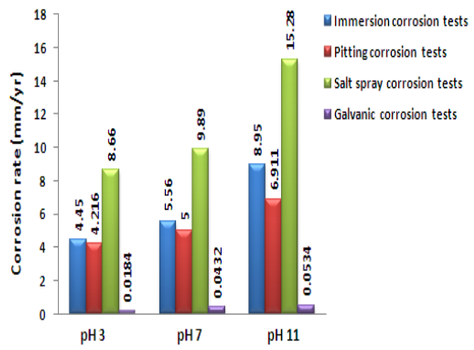

Fig. 6 Comparative estimation of corrosion rate with respect to Chloride ion concentration.

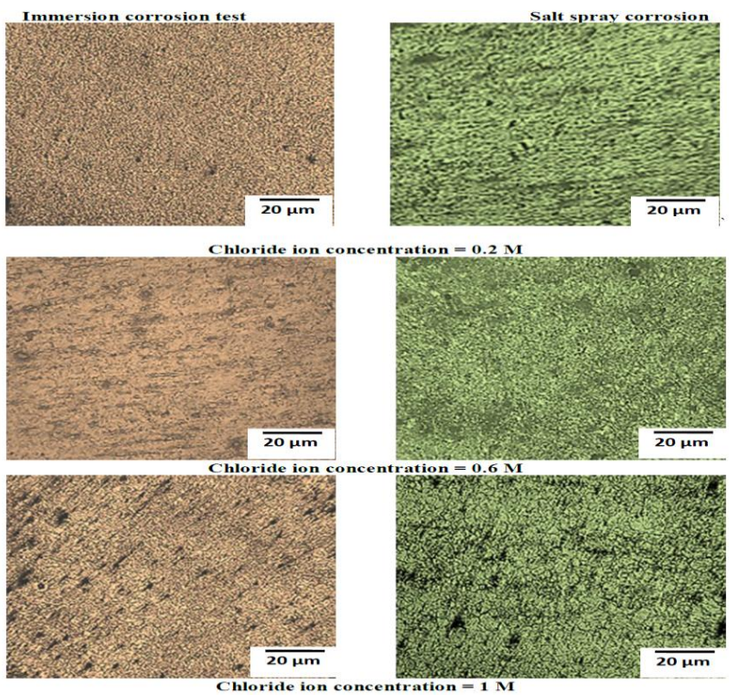

Fig. 7 Effect of Chloride ion concentration on Pit Morphology for immersion corrosion tests and salt spray corrosion tests

Fig. 7 shows the effect of Chloride ion concentration on pit morphology of the corroded specimen exposed in pH 7 for 5 hours with different chloride ion concentration of 0.2M, 0.6Mand 1M immersion corrosion tests and salt spray corrosion tests. During salt spray testing, it showed that the alloy exhibited a rise in corrosion rate with the increase in Cl^- concentration and thus the change of Cl^- concentration affected the corrosion rate much more in higher concentration solutions than that in lower concentration solutions. When more Cl^- in NaCl solution promoted the corrosion, the corrosive intermediate (Cl^-) would be rapidly transferred through the outer layer and reached the substrate of the alloy surface. Hence, the corrosion rate was increased [23]. While in immersion corrosion tests, the specimen exhibited a rise in corrosion rate with increase in Cl^- concentration and thus the change of Cl^- concentration affected the corrosion rate much more in higher concentration solutions than that in lower concentration solutions. But the rising rate of corrosion with the increase of chloride ion concentration was reduced in both immersion and polarization tests.

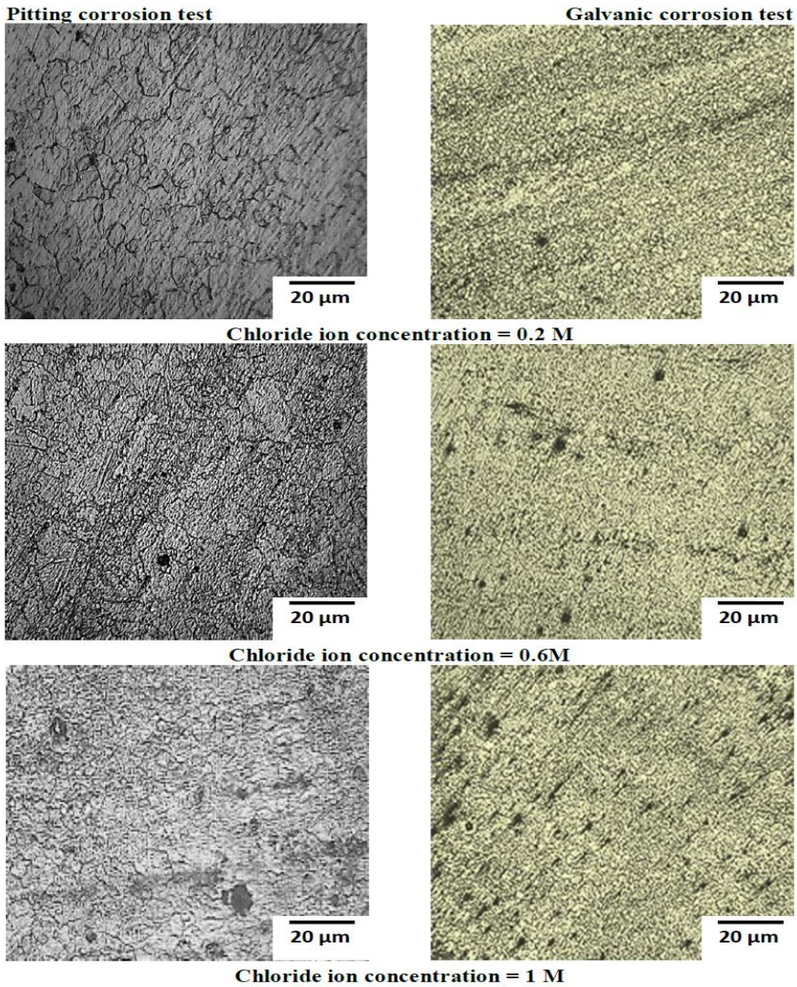

Fig.8 Effect of Chloride ion Concentration Pit Morphology for pitting corrosion tests and galvanic corrosion tests.

Fig. 8 shows the effect of Chloride ion concentration on pit morphology of the corroded specimen exposed in pH 7 for 5 hours with different chloride ion concentration of 0.2M, 0.6Mand 1M pitting corrosion tests and galvanic corrosion tests. During pitting corrosion tests, the chloride ion tends to be concentrated inside the pit causing anodic dissolution of magnesium, not the surface of the substrate. Thus the rising rate of corrosion was reduced with the increase in chloride ion concentration. As the microscopic view, the rising of corrosion rate was reduces with the increase of the chloride ion concentration leads to the conclusion that the β-phase was more stable in NaCl solution and was more inert to corrosion; the β-phase was itself, however, an effective cathode. Thus, the rising rate of the corrosion was reduced with the increase of chloride ion concentration. Chloride ions were aggressive for magnesium. Concerning about the pit characteristics, more number of pits were observed in the specimen exposed to immersion and polarization test than the salt spray test. This can be explained by the exposure environment. The exposed surfaces during immersion and polarization test were continuously exposed to dissolved chloride ions, meaning new pits could form at any point. The ability of the pits to form whenever desired on the polarized surfaces means that depth would not be affected. However, because pits could only form during chloride ion exposure period on the salt spray surfaces, the time separating the exposure would be a major determining force in pit depth. The chloride ions are more aggressive to the magnesium alloys. Since increase in the chloride ion concentration enhance the corrosion behavior in all the four corrosion tests. It was obvious from the observation of pit number densities, which increases with the increase in chloride ions.

During galvanic corrosion tests, the pit morphology described that the pit formation depends on the change in the chloride ion concentration of the solution. Here, with the increase of chloride ion concentration of the solution, the density of the pit increases. Thus, corrosion rate to be increased with increasing chloride ion concentration. The anodic specimen exhibited a rise in corrosion rate with increase in Cl^- concentration and thus the change of Cl^- concentration affected the corrosion rate much more in higher concentration solutions than that in lower concentration solutions. When more Cl^- in NaCl solution promoted the corrosion, the corrosive intermediate (Cl^-) would be rapidly transferred through the outer layer and reached the substrate of the alloy surface. Hence, the corrosion rate was increased [30].

5.3 Effect of corrosion time on corrosion rate

On comparison, the corrosion rates among the four corrosion tested specimen were represented as bar diagram in the Fig. 9. With the increase of corrosion time the corrosion rate decreases for the specimens undergone four corrosion tests. It proved that the protective layer made a predominant role to strike against corrosion with the increment of time. The corrosion rate seems higher in salt spray corrosion test due to the spraying effect, while in exposed condition, the protective layer formed during immersion and polarization test was enhanced by the alkalization of the solution.

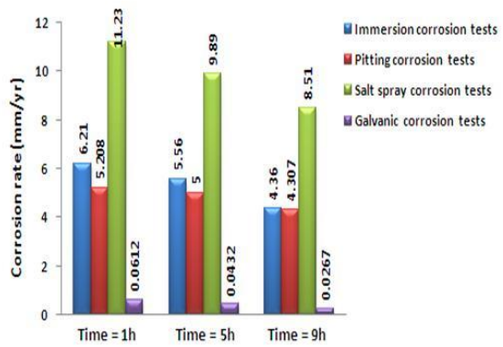

Fig. 9 Comparative estimation of corrosion rate with respect to corrosion time.

Fig. 10 & Fig.11 shows the effect of corrosion time on pit morphology of the corroded specimen exposed in pH 7 with chloride ion concentration of 0.6M NaCl exposed 1h, 5h and 9h immersion corrosion tests and salt spray corrosion tests. The mode of microstructural features was comparatively same during corrosion testing for immersion, salt spray, pitting and galvanic corrosion tests as its corrosion time taken into an account. The FS welded specimens possess refined grain and quite a lot of β particles were distributed along the grain boundary. In this case, β phase particles cannot be easily destroyed and, with the increase of corrosion time, the quantity of β phases in the exposed surface would increase and finally play the role of corrosion barrier [31]. Although, there are some grains of α phase still being corroded, most of the remaining α phase grains are protected under the β phase barrier, so the corrosion rate decreased with the increase in corrosion time. Thus the corrosion morphology of the alloy was predominantly controlled by the β phase distribution [32]. As seeing the pit number density, both the tested specimen begins decline in its count of the pits. The distance between the pits were increased, meaning that,

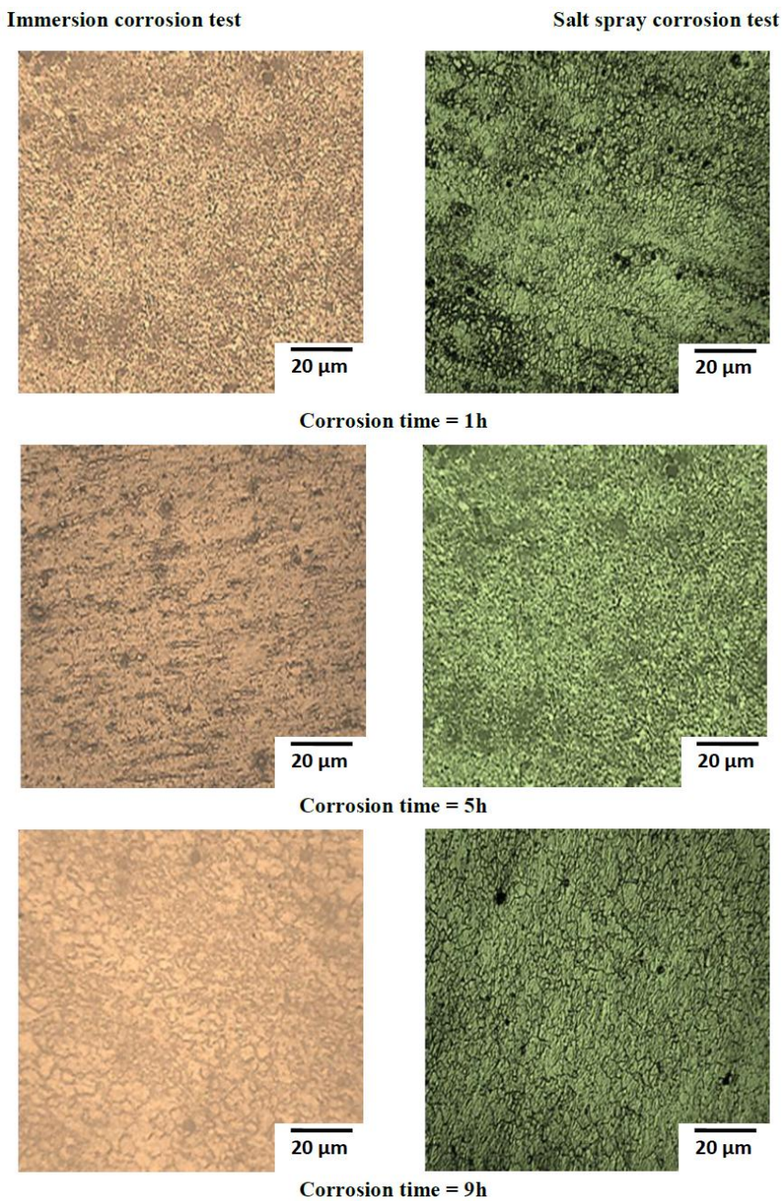

Fig. 10 Effect of Corrosion time on Pit Morphology for immersion corrosion tests and salt spray corrosion tests

the pit area was highly protected with the magnesium hydroxide layer, and also, uninhibited by general corrosion removing magnesium surrounding the pit. It results an increase in hydrogen evolution with the increasing corrosion time, which tends to increase the concentration of insoluble corrosion products $Mg(OH)_2$. The insoluble corrosion products on the surface of the alloy could slow down the corrosion rate for all the four corrosion tests. On comparison among the four corrosion tests, the corrosion mechanisms seem identical for different corrosion tests underwent for stir welds. This helps to find an easier corrosion resistant method to suppress the corrosion of stir welded magnesium alloy. Also, from the results it shows that areas under stir

welding possess equivalent strength to the base metal as for other welding process. Hence, improvements in mechanical properties and corrosion resistance of magnesium alloy have led to greater interest in magnesium alloys for structural, automobile, aerospace and specialty applications.

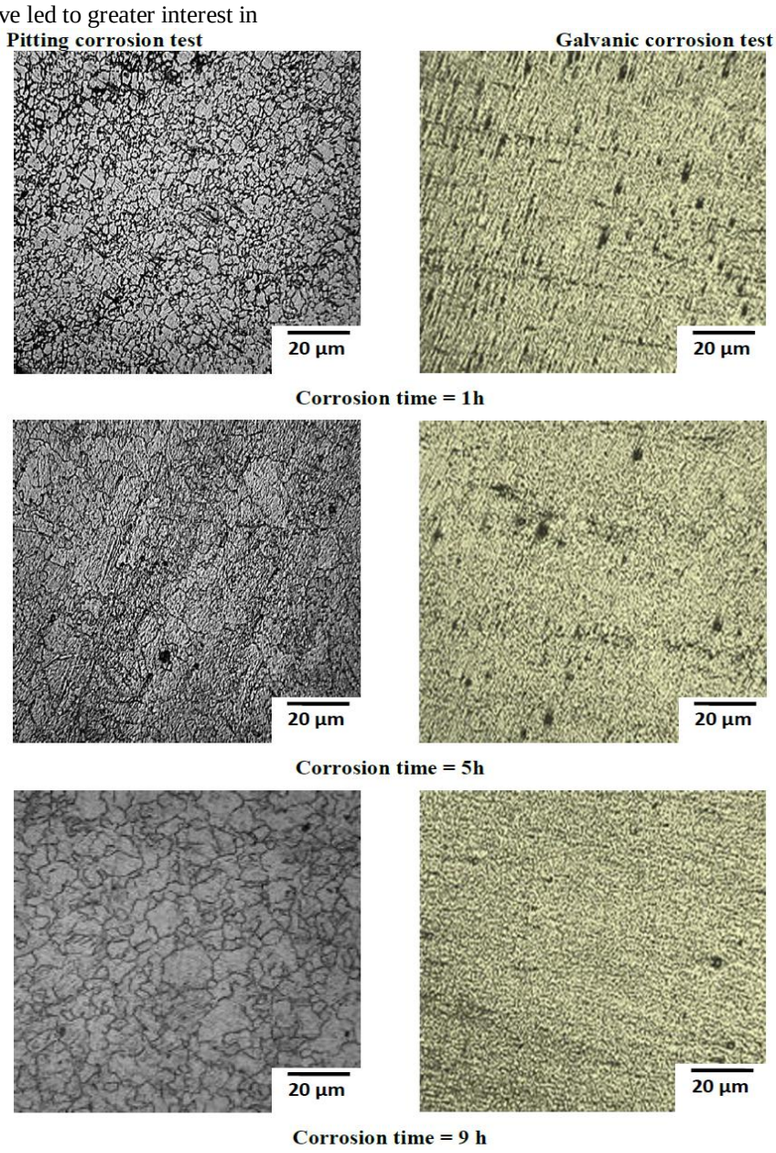

Fig.11 Effect of corrosion time on Pit Morphology for pitting corrosion tests and galvanic corrosion tests.

6. Conclusions

From the corrosion survey, finally the following quantitative and characterization inference were observed on AZ31B magnesium alloy welds;

The corrosion rate was higher in salt spray corrosion tests than the immersion, pitting and galvanic corrosion tests. This is due to the fact; there is a substantial increase in the pH during immersion, pitting and galvanic corrosion test as the specimen exposed throughout the test. But, in salt spray test, the electrolyte was freshly used and not recycled. Therefore it eliminates the basification/alkalization in the solution.

The corrosion rate was decreased with increasing pH value due to the formation hydroxide layer, which in turns restrain the corrosion further. It was observed that, low corrosion rate was found in alkaline conditions in all the four corrosion tests. So it was suggested that AZ31B magnesium alloy welds hold a best service applications in alkaline environment.

It results an increase in hydrogen evolution with the increasing corrosion time, which tended to increase the concentration of OH^- ions thereby increasing fraction of the surface was observed, which is the insoluble corrosion products $Mg(OH)_2$. The insoluble corrosion products on the surface of the alloy could slow down the corrosion rate for all the four corrosion tests.

The chloride ions are more aggressive to the magnesium alloys. Since increase in the chloride ion concentration enhance the corrosion behavior in all the four corrosion tests. It was obvious from the observation of pit number densities, which increases with the increase in chloride ions.

The corrosion rate was differs in four different tests. However, a slight variation in between the immersion and the pitting corrosion tests, since it possesses same mode of corrosion and found with respect to the order as Salt spray corrosion tests > Immersion corrosion tests > Pitting corrosion tests > Galvanic corrosion tests. Also, the results it shows that areas under stir welding possess equivalent strength to the base metal as for other welding process.

Acknowledgement

The authors would like to thank Centre for Materials Joining & Research (CEMAJOR), Department of Manufacturing Engineering, Annamalai University, Annamalai Nagar, for extending the facilities of Materials Joining Laboratory and Corrosion Testing laboratory to carry out this investigation.

References

1. *Modike B.L and Ebert T (2001) "Magnesium – Properties, Applications, Potential", Mater. Sci. and Engg. A, Vol. 302 37-45.*
2. *Zeng R.C, Dietzel W, Zettler R, Chen J and Kainer K.U (2008)," Trans. of Non-Ferr.", Met. Soc. of China, Vol.18, 76-80.*
3. *Zeng R.C, Zhang J, Huang W.J, Dietzel W, Kainer K.U, Blawert C, and Ke W (2006), "Trans. of Non-Ferr.", Met. Soc. of China Vol.16,763-771.*
4. *Nagasawa T, Otsuka M, Yokota T and Ueki T (2000), "Structure and Mechanical Properties of Friction stir Weld Joints of Magnesium alloy AZ31; in: H.I Kaplan, J. Hryn, B. Clow [Eds.] Magnesium Technology 2000", TMS, Warrendale 383-387.*
5. *Weifeng X, Liu J, Zhu H (2011), "Pitting corrosion of friction stir welded aluminium alloy thick plate in alkaline chloride solution", Trans. of Non-Ferr. Met. Soc. of China Vol.21, 188-193*
6. *Zhao M and Wu S (2006), "A Chromium free conversion coating of magnesium alloy by a phosphate permanganate solution", Surf. Coat and Tech. Vol.200, 5407-5412.*
7. *Altun H and Sadrisen (2004), "Studies on the influence of chloride ion concentration and pH on the corrosion of AZ63 magnesium alloy", Mater. And Des. Vol.25, 637-641.*
8. *Song Y, Shan D, Chen R and Han E (2010), "Effect of second phases on the corrosion behavior of wrought Mg-Zn-Y-Zr alloy", Corr. Sci. Vol.52, 1830-1837.*
9. *Dhanapal A, Rajendra Boopathy S and Balasubramanian V (2011), "Developing an empirical relationship to predict the corrosion rate of friction stir welded AZ31B magnesium alloy under salt fog environment", Mater. And Des., Vol.32, 5066-5072.*
10. *Box G.E.P and Draper N.R (1987), "Empirical Model Building and Response Surface", John Wiley and Sons, New York.*
11. *ASM International, Metals Handbook, Corrosion, ninth ed., ASM International, 1987.*
12. *Jones D.A (1992), "Principles and Prevention of Corrosion", Prentice-Hall, Englewood Cliffs, NJ.*
13. *Fontana M.G and Greene N.D (1984), "Corrosion Engineering", McGraw-Hill, New York.*
14. *Uhlig H.H (1973), "Corrosion and Corrosion Control", Wiley, New York.*
15. *Song G, Atrens A, St. John D and Hryn J.N (2001), "Magnesium Technology 2001 Symposium", Minerals, Metals & Materials Society, New Orleans, LA, 255–262.*
16. *Zhao M.C, Liu M, Song G and Atrens A (2008), "Influence of the beta-phase morphology on the corrosion of the Mg alloy AZ91", Corr. Sci. Vol.50, 1939–1953*
17. *Zhao M.C, Liu M and Song G (2008), "Influence of microstructure on corrosion of as-cast ZE41", Adv. Engg. Mater. Vol. 10, 104–111.*
18. *Zhao M.C, Schmutz P, Brunner S, Liu M, Song G and Atrens A (2009), "An exploratory study of the corrosion of Mg alloys during interrupted salt spray testing", Corr. Sci. Vol.51, 1277–1292.*
19. *Kok-Hui Goh, Teik-Thye Lim and Peng Chui (2008), "Evaluation of the effect of dosage, pH and contact time on high-dose phosphate inhibition for copper corrosion control using response surface methodology (RSM)", Corr. Sci. Vol.50, 918-927.*
20. *Aslan N (2008), "Application of response surface methodology and central composite rotatable design for modeling and optimization of a multi gravity separator for chromite concentration", Powd. Tech, Vol.185,80-86.*
21. *Bruce D Craig (1995), "Handbook of Corrosion Data", ASM International.*

22. *Uhlig H (1948), "The Corrosion Handbook", J. Wiley Publication, New York.*
23. *Babion R (2005), "Corrosion tests and standards: Application and Interpretation", ASTM international.*
24. *Peng L, Chang J, Guo X, Atrens A, Ding W and Peng Y, "Influence of heat treatment and microstructure on the corrosion of magnesium alloy Mg–10Gd–3Y–0.4Zr", J. of Appl. Electrochem., doi:10.1007/s10800-008-9739-4.*
25. *Song G and Atrens A(1999), "Corrosion mechanisms of magnesium alloys", Adv. Engg. Mater. Vol.1, 11–33.*
26. *Zeng R.C, Chen J, Dietzel, Zettler R., Santos J.F, Nascimento L and Kainer K. U (2009), "Corrosion of friction stir welded magnesium alloy AM50", Corrosion Science, Vol.51, 1738-1746.*
27. *Rose R, Manisekar K. and Balasubramanian V (2011), "Effect of axial force on microstructure and tensile properties of friction stir welded AZ31B magnesium alloy", Transactions of Non-ferrous Metals Society of China, Vol. 16, 974-984.*
28. *Holly J Martin, Horstemeyer M.F, Paul T Wang (2011), "Quantification of corrosion mechanisms under immersion and salt-spray environments on an extruded AZ31 magnesium alloy", Corr. Sci. Vol.53, 1348-1361.*
29. *Song G (2005), "Recent Progress in Corrosion and Protection of Magnesium Alloys", Adv. Engg. Mater. Vol.7, 563.*
30. *Hara N, Kobayashi Y, Kagaya D and Akao N (2007), "Formation and breakdown of surface films on magnesium and its alloys in aqueous solutions", Corr. Sci. Vol.49, 166-175.*
31. *Zhi-min Z, Xu H and Cheng L (2010), "Corrosion properties of plastically deformed AZ80 magnesium alloy", Tran. Of Non-ferr. Met. Soc. China, Vol. 20, 697-702.*
32. *Wang L, Zhang B and Shinohara T (2010), "Corrosion Behaviour of AZ91Magnesium alloy in dilute*